Article

A Study on Correlation between Ultrasonic Pulse Velocity Method and Coarse Aggregate for Estimating Residual Modulus of Elasticity of Concrete Exposed to High Temperatures

Wonchang Kim [1],[†], Keesin Jeong [1],[†], Taegyu Lee [1],[*] and Sungyu Park [2],[*]

[1] Department of Fire and Disaster Prevention, Semyung University, Jecheon 27136, Korea; kimwc69082@gmail.com (W.K.); jks@semyung.ac.kr (K.J.)
[2] Department of Architectural Engineering, Mokwon University, 88 Doanbukro, Seogu, Daejeon 35349, Korea
[*] Correspondence: ltg777@semyung.ac.kr (T.L.); psg@mokwon.ac.kr (S.P.); Tel.: +82-43-649-1315 (T.L.); +82-42-829-7712 (S.P.)
[†] These authors contributed equally to this work as first author.

Abstract: In this study, the mechanical properties of normal concrete (NC) and lightweight concrete (LC) were measured upon exposure to high temperatures (20, 100, 200, 300, 500, and 700 °C). Then, analysis was conducted to predict the residual modulus of elasticity through ultrasonic pulse velocity. Crushed granite aggregate was mixed as the coarse aggregate for NC and coal-ash aggregate for LC. The effect of the water-to-binder (W/B) ratio (0.41, 0.33, and 0.28) on the mechanical properties (residual compressive strength, residual ultrasonic pulse velocity, residual modulus of elasticity, and stress–strain) of concrete was determined. The residual compressive strength, residual ultrasonic pulse velocity, and residual modulus of elasticity were higher for LC compared to NC. The correlation between the ultrasonic pulse velocity and residual modulus of elasticity was also analyzed, which yielded a high correlation coefficient (R^2) at all levels. Finally, equations for predicting the residual modulus of elasticity using ultrasonic pulse velocity with R^2 values of 0.94 and 0.91 were proposed for NC and LC, respectively.

1. Introduction

Building fires occur more frequently than other fires, causing considerable property damage and human casualties [1]. This has prompted extensive research on reducing fire damage in buildings. Several major factors are responsible for the degraded mechanical properties of concrete buildings exposed to fire. Accelerated carbonation by the dehydration of calcium hydroxide ($CaOH_2$) in concrete and microcracks caused by the different thermal expansion properties of aggregate and paste significantly degrade concrete durability. In addition, long-term exposure to high temperatures causes porosity and significant cracking because of the chemical decomposition of the concrete matrix, resulting in significant deterioration in the structural performance [2–4]. Therefore, this warrants the accurate measurement of the mechanical properties of concrete after exposure to fire, which can enable the accurate assessment of repair or demolition, thereby saving cost and time, as well as reducing additional human casualties and property damage caused by secondary collapse [5–7].

The most accurate method to characterize the mechanical properties of a building degraded after fire is the direct destructive test of the degraded concrete members. Core extraction for the destructive test of the degraded members is required for building fire safety diagnosis, which presents the following problems: (1) core extraction and destructive testing is expensive and (2) continuous research is necessary to address problems with

equipment, manpower, and time required. Thus, building safety diagnosis and assessment through non-destructive methods are preferred today. Among the several non-destructive methods, ultrasonic pulse velocity method is proposed as a method to estimate mechanical properties in this study. The ultrasonic pulse velocity is a function of the time and distance that the ultrasonic pulse transmitted from the transmitting transducer measures the time when it arrives at the receiving transducer and represents a value since it shows different tendencies depending on the internal structure and defects of the concrete, it has a high possibility in predicting defects according to the internal state of the concrete. The equipment of this method is portable, while safety diagnosis does not require expert skills and can be performed at a relatively low cost and in short time, compensating for the drawbacks of destructive testing. Several studies on predicting the mechanical properties of concrete through ultrasonic pulse velocity analysis after high temperature exposure have been reported [8–11].

However, these have focused on compressive strength prediction, with limited information on the prediction of the modulus of elasticity, i.e., stiffness, which is an equally important for accurate safety diagnosis of fire-damaged concrete. The residual modulus of elasticity of concrete after high temperature exposure varies depending on the aggregate type [12] (Figure 1). Since the modulus of elasticity is significantly affected by the stiffness of the coarse aggregate, it is necessary to consider the aggregate type to accurately predict the residual modulus of elasticity of concrete after high temperature exposure [13–15]. The ultrasonic pulse velocity is significantly affected by the materials mixed in concrete, including the aggregate [16]. Therefore, the ultrasonic pulse velocity method that considers the influence of the aggregate type is expected to be suitable for accurately measuring the residual modulus of elasticity after high temperature exposure.
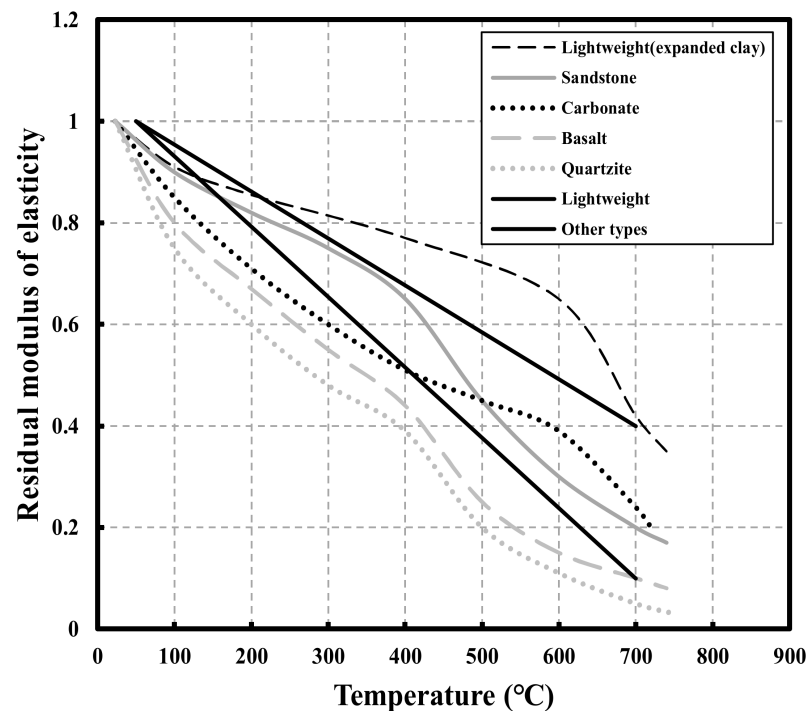
Figure 1. Residual modulus of elasticity according to type of aggregate after high temperature exposure.

In this study, the mechanical properties of concrete mixed with normal aggregate (normal concrete (NC)) and lightweight aggregate (lightweight concrete (LC)) were evaluated at various water-to-binder (W/B) ratios (0.41, 0.33, and 0.28). The amount of cement and aggregate mixed varies according to the W/B ratio. It is necessary to consider W/B because the ultrasonic velocity shows a different tendency depending on the material mixed in the concrete. In addition, experimental results have been reported that concrete exhibits different mechanical properties depending on W/B at previous high temperatures, and it is

judged that W/B should be considered to accurately measure the degradation of different mechanical properties with ultrasonic pulse velocity. In addition, residual mechanical properties (residual compressive strength, residual ultrasonic pulse velocity, and residual modulus of elasticity) and stress–strain were measured at varying temperatures. After measurement, the correlation between the ultrasonic pulse velocity and residual modulus of elasticity was analyzed according to the W/B ratio for NC and LC. Finally, equations for predicting the residual modulus of elasticity using ultrasonic pulse velocity after high temperature exposure were proposed for NC and LC, respectively.

2. Materials and Methods

2.1. Materials

Table 1 shows the physical properties of the materials used in this study. Type 1 ordinary Portland cement (OPC) with a density of 3150 kg/m^3 and a fineness of 320 m^2/kg was used. Two types of coarse aggregates, crushed granite aggregate and coal-ash aggregate were used. The density, fineness modulus, absorption, and maximum size of the crushed granite aggregate were 2680 kg/m^3, 7.03, 0.68%, and 20 mm, respectively, while those of the coal-ash aggregate were 1470 kg/m^3, 6.39, 8.68%, and 20 mm, respectively. River sand was used as the fine aggregate with a density, fineness modulus, and absorption of 2540 kg/m^3, 2.54, and 1.6%, respectively. In addition, polycarboxylic-based acid was used as a superplasticizer. Table 2 shows the chemical properties of the cement.

Table 1. Physical properties of the materials.

Properties	Cement (Type I Ordinary Portland Cement)	Coarse Aggregate		Fine Aggregate	S.P
		Granite	Coal-Ash		
Density (kg/m^3)	3150	2680	1470	2540	Polycarboxylic-based acid
Fineness (m^2/kg)	320	-	-	-	
Fineness modulus	-	7.03	6.39	2.54	
Absorption (%)	-	0.68	8.68	1.6	
Maximum size (mm)	-	20	20	-	

S.P: Super plasticizer.

Table 2. Chemical properties of cement.

Chemical Composition (%)	OPC
CaO	60.34
SiO$_2$	19.82
Al$_2$O$_3$	4.85
Fe$_2$O$_3$	3.30
MgO	3.83
SO$_3$	2.88
K$_2$O	1.08
Others	0.86
L.O.I.	3.02

(1) OPC: ordinary Portland cement; (2) L.O.I.: loss on ignition.

2.2. Proportions of the NC and LC Mixtures

The W/B ratios were set to 0.41, 0.33, and 0.28 for NC and LC and their mechanical properties analyzed at various strengths after high temperature exposure (Table 3; in the 'Mix ID', the numbers written after NC and LC represent the W/B ratio). Crushed granite aggregate was used as the coarse aggregate for NC and coal-ash aggregate for LC and their

effect on the mechanical properties determined. The cement, water, and fine aggregate contents were kept constant under the same W/B ratio.

Table 3. Mix proportions of normal concrete (NC) and lightweight concrete (LC).

Mix ID	NC41	LC41	NC33	LC33	NC28	LC28
Water/Binder	0.41	0.41	0.33	0.33	0.28	0.28
Sand/aggregate (%)	46.0	46.0	43.0	43.0	43.0	43.0
Water (kg/m^3)	165	165	165	165	165	165
Cement (kg/m^3)	400	400	500	500	600	600
Fine aggregate (kg/m^3)	799	799	711	711	676	676
Granite aggregate (kg/m^3)	956	-	961	-	913	-
Coal-ash aggregate (kg/m^3)	-	758	-	762	-	724

2.3. Experimental Parameters and Test Methods

The effect of the coarse aggregate type (crushed granite aggregate in NC vs. coal-ash aggregate in LC) and W/B ratio (0.41, 0.33, and 0.28) on the ultrasonic pulse velocity and other mechanical properties of concrete after high temperature exposure was evaluated. Cylindrical specimens (d × h = 100 × 200 mm) were prepared, and were subjected to water curing for 28 days, followed by conditioning at 20 ± 2 °C and 60 ± 5% humidity for 91 days [17].

Table 4 shows the experimental procedure of this study. Figure 2 shows the electric furnace used for heating the specimens. The target temperature was set to 20, 100, 200, 300, 500, and 700 °C, and a low heating rate of 1 °C/min was applied as recommended by RILEM. Once the target temperature was reached, it was maintained for 60 min to ensure uniform heating inside and outside the specimen. The specimen was then subjected to dry air cooling for 24 h at room temperature. After cooling, the specimens were subjected to testing for residual compressive strength, residual ultrasonic pulse velocity, and residual modulus of elasticity.

Table 4. Experimental parameters.

ID	Type of Coarse Aggregate	W/B	Heat Method	Curing	TEST ITEM
NC	Crushed granite aggregate	0.41 0.33	23, 100, 200, 300, 500, 700 °C	Water curing Room temperature (20 ± 2 °C)	Residual compressive strength Residual ultrasonic pulse velocity
LC	Coal-ash aggregate	0.28	(1 °C/min)	Humidity (60 ± 5%)	Residual modulus of elasticity

Figure 2. Electric furnace.

The compressive strength and modulus of elasticity were measured as shown in Figure 3, in accordance with ASTM C39/C39M and ASTM C469 [18,19], respectively. The ultrasonic pulse velocity was measured as shown in Figure 4, in accordance with ASTM C597 and calculated using Equation (1) [20]. All residual mechanical properties were calculated using Equation (2) (Table 5).

Figure 3. Compressive strength and elastic modulus test.

**Figure 4.** Ultrasonic pulse velocity test.

Table 5. Testing of residual mechanical properties.

Test Items	Test Method	Equation (1)	Equation (2)
Residual compressive strength Residual modulus of elasticity Residual ultrasonic pulse velocity	ASTM C39/C39M ASTM C469 ASTM C597	$V_p = \frac{L}{t}$ V_p: ultrasonic pulse velocity(m/s) L: distance(m) t: time(s)	$M_{re} = \frac{M_R}{M_T}$ M_{re}: residual mechanical properties M_R: mechanical properties at room temperature M_T: mechanical properties at high temperature

3. Results and Discussion

3.1. Residual Mechanical Properties of NC and LC after High Temperature Exposure

Figure 5 shows the compressive strength of NC and LC after high temperature exposure. At 100 °C, NC41 and NC33 showed a residual compressive strength of approximately 0.91, which was slightly higher for LC41 and LC33 at approximately 0.96. At a W/B ratio of 0.28, the residual compressive strength was relatively lower compared to the other W/B ratios, resulting in 0.86 for NC28 and 0.89 for LC28. For all specimens, strength degradation was observed until 200 °C, which slightly increased at 200–300 °C. The strength for all specimens increased by approximately 3%, except for NC28, which can be attributed to the influence of the forced hydration reaction caused by the evaporation of free water inside the specimen at high temperature and the influence of the stress and vapor pressure caused by the thermal expansion of the aggregates [21–23].
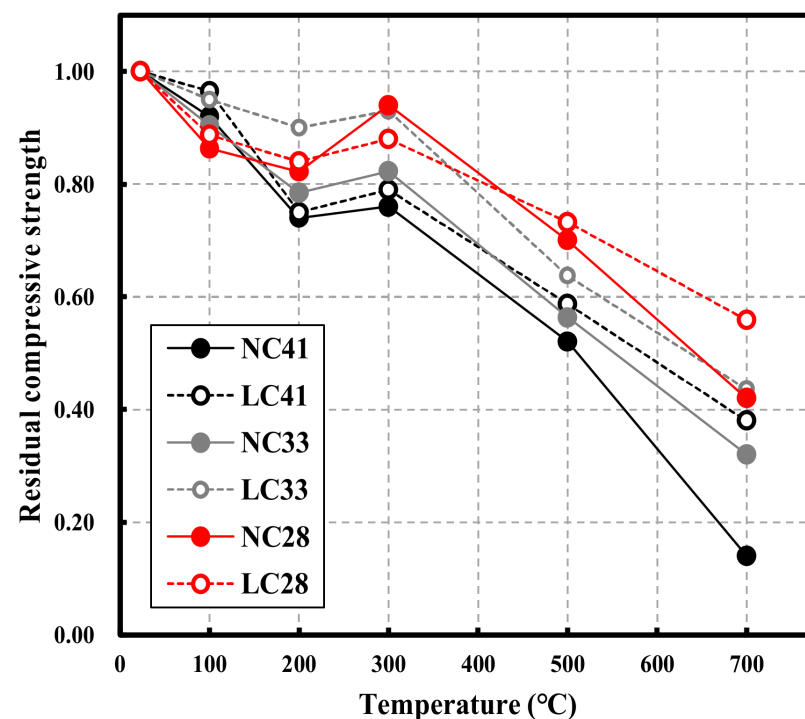

Figure 5. Residual compressive strength of normal concrete (NC) and lightweight concrete (LC) after high temperature exposure.

Above 300 °C, the strength continuously decreased, leading to a rapid strength loss above 400 °C. This was because of the severe matrix damage caused by the decomposition of C-S-H, the main component of hardened cement. Above 500 °C, LC exhibited a higher residual compressive strength than NC at all levels. NC41, NC33, and NC28 showed residual compressive strengths of 0.52, 0.56, and 0.70, respectively, while LC41, LC33, and LC28 exhibited 0.59, 0.64, and 0.73, respectively. At 700 °C, the residual compressive strengths of NC and LC showed the largest difference. NC41, NC33, and NC28 showed residual compressive strengths of 0.14, 0.32, and 0.41, respectively, while LC41, LC33, and LC28 exhibited 0.38, 0.44, and 0.56, respectively. It appears that the relatively small thermal expansion after high temperature exposure caused by the porosity of the coal-ash aggregate

mixed in LC improved the stress at the paste–aggregate interface [24,25]. Microanalysis has shown that the stress at the paste–lightweight aggregate interface is stronger compared to that at the paste–normal aggregate interface [26].

Figure 6 shows the residual ultrasonic pulse velocity of NC and LC after high temperature exposure. Unlike the residual compressive strength, the residual ultrasonic pulse velocity showed a tendency to linearly decreased as the temperature increased. At 100 °C, the residual ultrasonic pulse velocity was approximately 0.97% at all levels, showing a higher residual rate compared to the residual compressive strength. At 200 °C, the residual ultrasonic pulse velocities were found to be 0.83 and 0.86 for NC41 and LC41, respectively, 0.88 and 0.85 for NC33 and LC33, respectively, and 0.90 for both NC28 and LC28. At 300 °C, they were 0.75 and 0.79 for NC41 and LC41, respectively, 0.76 and 0.80 for NC33 and LC33, respectively, and 0.89 and 0.90 for NC28 and LC28, respectively. At temperatures higher than 300 °C, LC exhibited higher residual ultrasonic pulse velocities than NC.
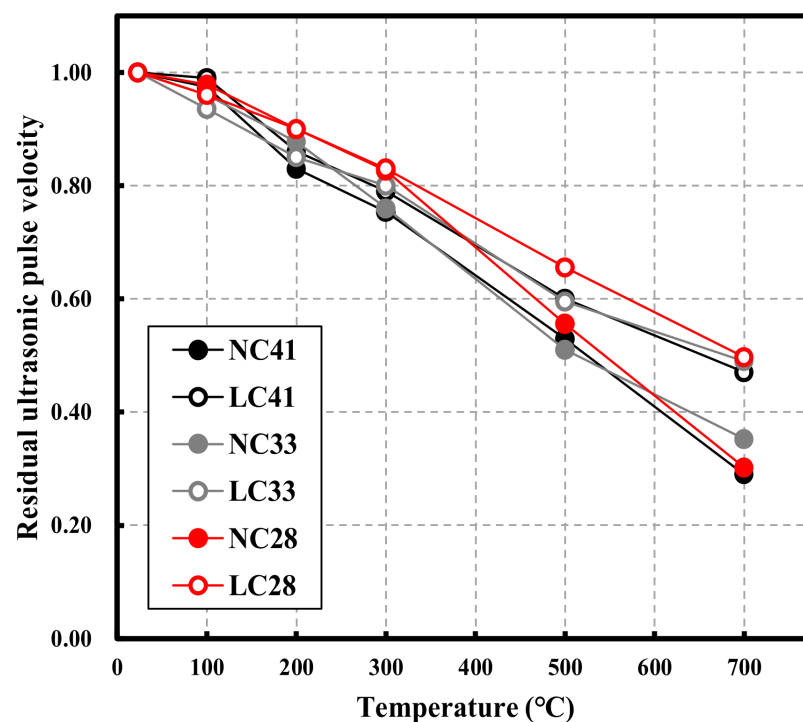

Figure 6. Residual ultrasonic pulse velocity of normal concrete (NC) and lightweight concrete (LC) after high temperature exposure.

As the temperature increased, the difference in the residual ultrasonic pulse velocity between NC and LC became larger. At 500–700°C, LC28 shows a sharp decrease compared to LC41 and LC33, where chemical decomposition of the cement matrix occurs actively in the temperature section, and it is judged that the ultrasonic pulse velocity decreases rapidly due to matrix damage in LC28 with a large amount of cement mixture. At 500 °C, NC41, NC33, and NC28 showed residual ultrasonic pulse velocities of 0.53, 0.51, and 0.56, respectively, while LC41, LC33, and LC28 exhibited 0.60, 0.60, and 0.66, respectively. At 700 °C, NC showed a residual ultrasonic pulse velocity of approximately 0.31 at all levels, while LC exhibited approximately 0.49. It appears that the influence of the coarse aggregate on the ultrasonic pulse velocity increases as the temperature increases, in a similar manner to its influence on the residual compressive strength.

Figure 7 shows the residual modulus of elasticity of NC and LC after high temperature exposure. As the temperature increased, the residual modulus of elasticity showed a tendency to continuously decrease in a similar manner to that of the ultrasonic pulse velocity [27]. In addition, the residual modulus of elasticity showed a lower residual rate at the same temperature compared to the other mechanical properties [25,28]. At 100 °C, the

residual modulus of elasticity was approximately 0.88 at all levels. At 200 °C, it significantly decreased to 0.69 at a W/B ratio of 0.41 and approximately 0.76 at the remaining levels. At 300 °C, it was 0.70 for NC28 and approximately 0.59 at the remaining levels. The sharp decrease in the modulus of elasticity at higher temperatures can be attributed to the chemical decomposition of C-S-H gel, as was the case for the residual compressive strength. At temperatures higher than 500 °C, the residual modulus of elasticity of LC tended to be higher than that of NC under the same W/B ratio. At 500 °C, NC41, NC33, and NC28 showed residual moduli of elasticity of 0.20, 0.21, and 0.29, respectively, while LC41, LC33, and LC28 exhibited 0.30, 0.29, and 0.28, respectively. At temperatures below 700 °C, NC28 showed higher or similar residual moduli of elasticity compared to LC at all levels, but it exhibited a lower residual rate compared to LC at 700 °C. At 700 °C, NC41, NC33, and NC28 showed residual moduli of elasticity of 0.03, 0.05, and 0.09, respectively, resulting in very low residual rates, while LC41, LC33, and LC28 exhibited 0.14, 0.15, and 0.20, respectively. Although LC showed higher residual rates compared to NC, it appears that most of the stiffness disappeared at all levels at temperatures above 700 °C.
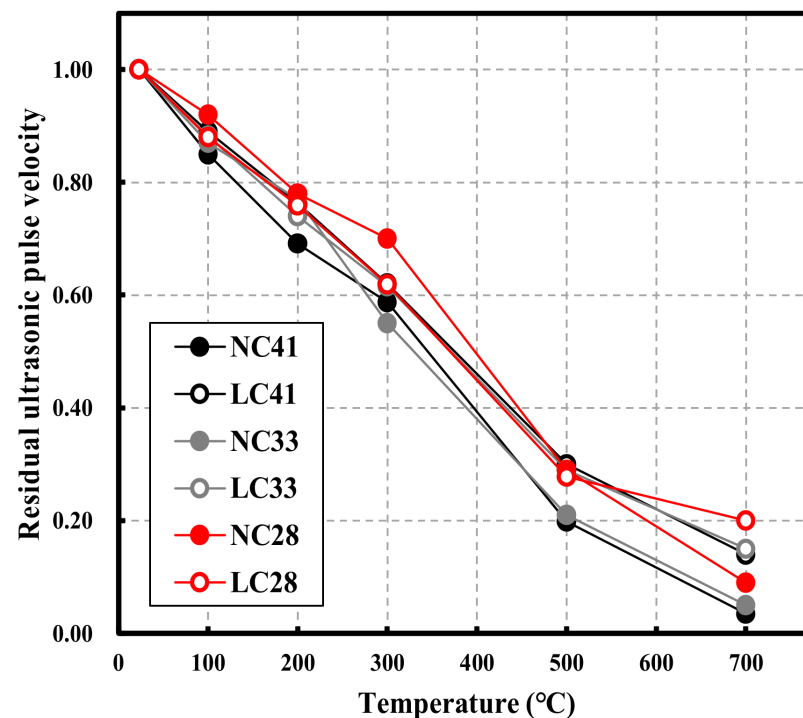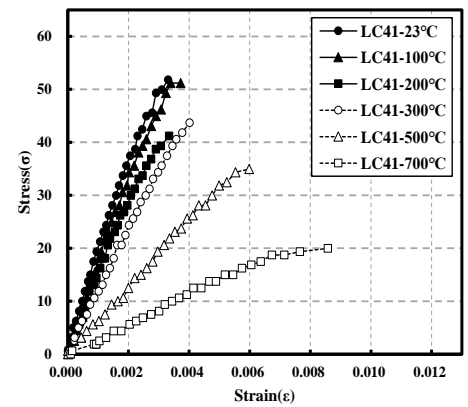

Figure 7. Residual modulus of elasticity of normal concrete (NC) and lightweight concrete (LC) after high temperature exposure.

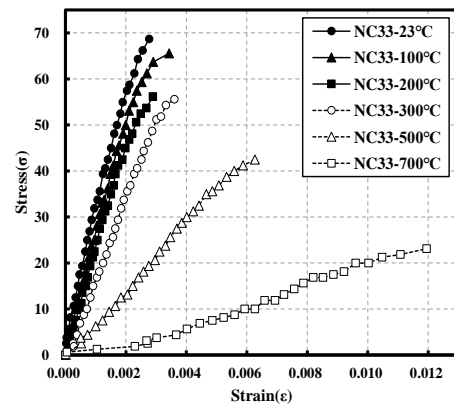### 3.2. Stress–Strain Analysis of NC and LC after High Temperature Exposure

Figure 8 shows the stress(σ)–strain(ε) curves of NC and LC after high temperature exposure. At all levels, the stress–strain curves in the temperature range below 300 °C showed slopes similar to that before heating (20 °C) [29,30]. While the strain of NC ranged from 0.0028 to 0.004 and that of LC from 0.0033 to 0.0042, brittle failure was observed in the temperature range below 300 °C. Considering that the failure strain of ordinary concrete ranges from 0.0025 to 0.004, the concrete heated up to 300 °C appears to have exhibited a tendency similar to that of concrete before heating. Above 500 °C, the slope of the stress–strain curve tended to decrease at all levels. At 700 °C, ductile failure occurred with a strain of approximately 0.01. NC showed a failure strain at a relatively higher stress compared to LC at the same target temperature, indicating that the stress at the aggregate–paste interface improved with crushed granite aggregate, which has a relatively high roughness [31].
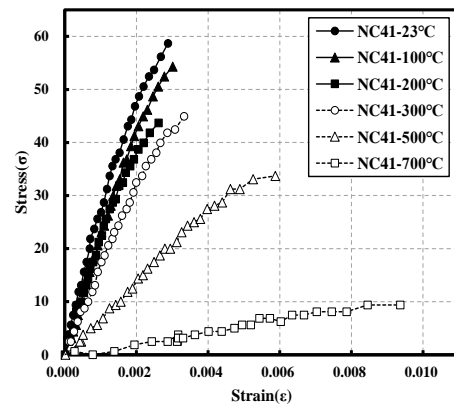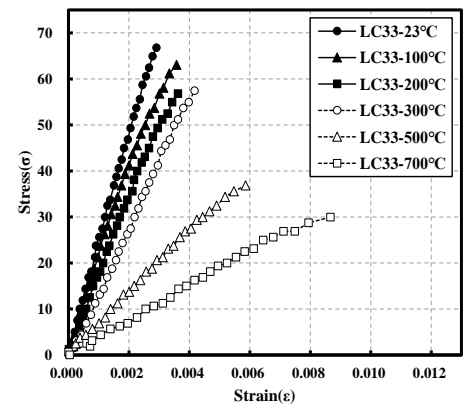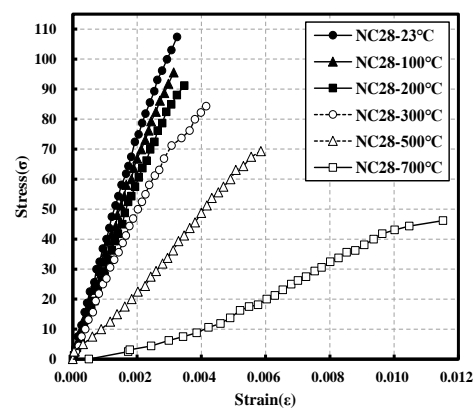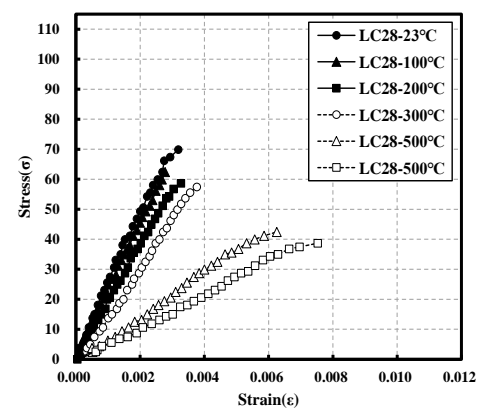
(**a**)

(**b**)

(**c**)

(**d**)

(**e**)

(**f**)
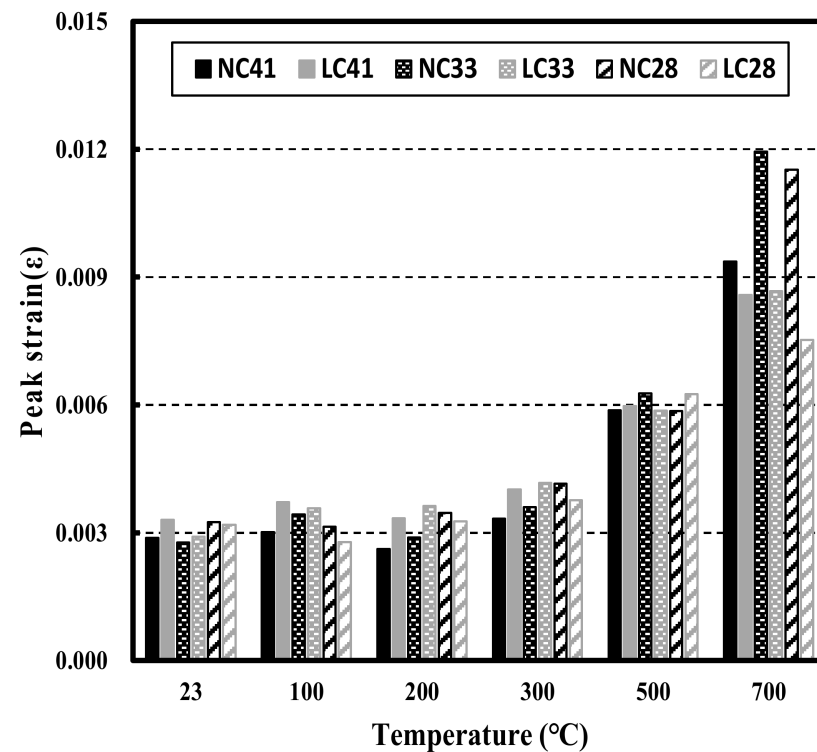
Figure 8. Stress(σ)–strain(ε) curves of normal concrete (NC) and lightweight concrete (LC) after high temperature exposure: (**a**) NC41; (**b**) LC41; (**c**) NC33; (**d**) LC33; (**e**) NC28; (**f**) LC28.

Figure 9 shows the peak strain of NC and LC after high temperature exposure. The strain showed a tendency to increase at all levels as the temperature increased, but a value (approximately 0.004) similar to that before heating (20 °C) was observed. In the

temperature range below 300 °C, LC41 and LC33 showed a higher peak strain than NC41 and NC33, whereas NC28 exhibited a higher peak strain than LC28. Above 500 °C, the peak strain sharply increased [32], ranging from 0.0058 to 0.0063 at 500 °C and from 0.0094 to 0.012 at 700 °C. At 700 °C, NC exhibited a higher peak strain than LC at all levels, indicating the significant influence of crushed granite aggregate with a relatively higher stiffness than that of coal-ash aggregate, which is more porous and of low density (see Table 1) [31].
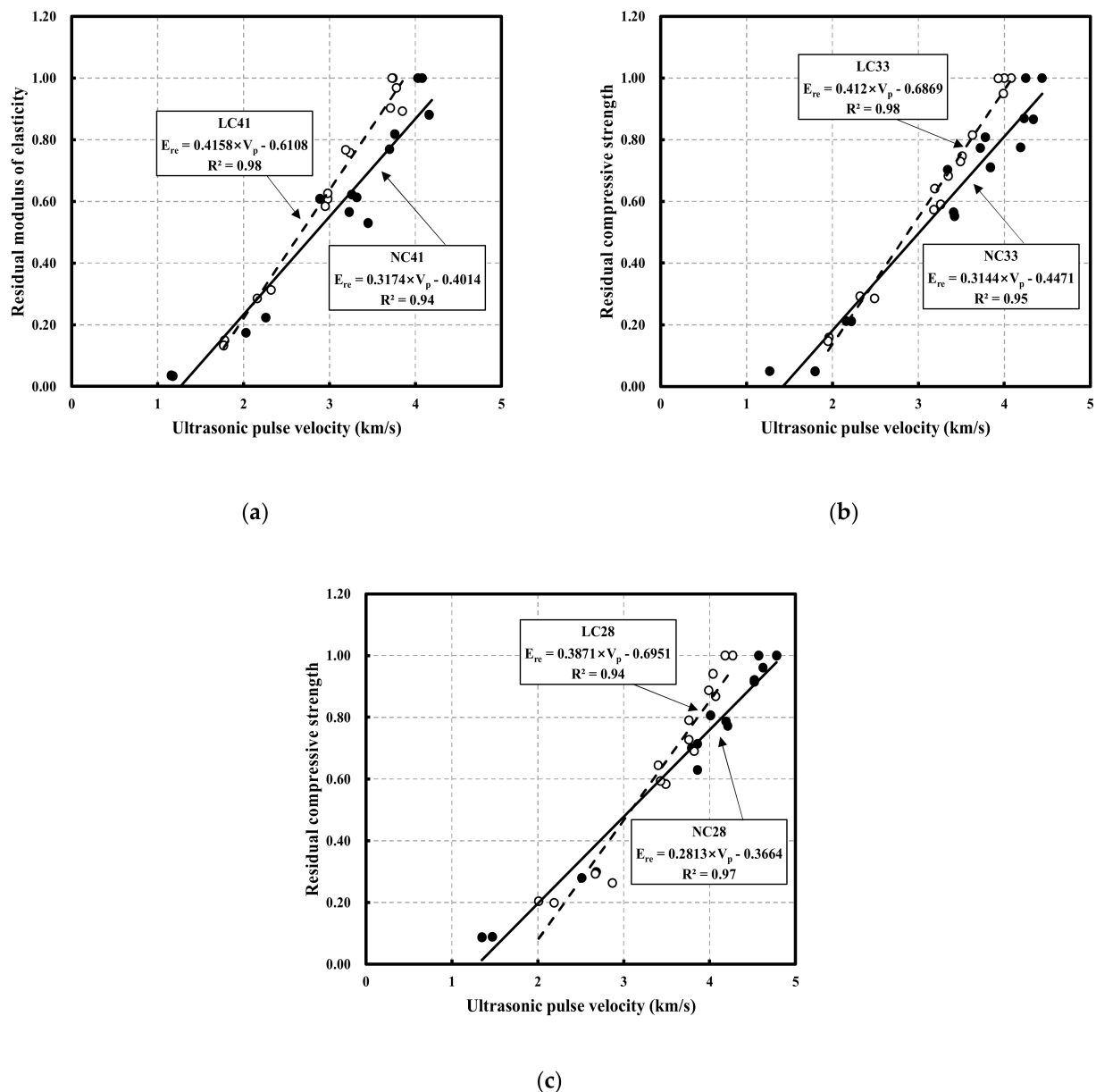

Figure 9. Peak strain of normal concrete (NC) and lightweight concrete (LC) after high temperature exposure.

3.3. Correlation between Ultrasonic Pulse Velocity and Residual Modulus of Elasticity of NC and LC after High Temperature Exposure

Figure 10 shows the correlation between the ultrasonic pulse velocity and residual modulus of elasticity of NC and LC after high temperature exposure according to the W/B ratio. A high correlation was observed in a linear graph, indicating that the tendencies of the ultrasonic pulse velocity and residual modulus of elasticity to linearly decrease with increasing temperature had a significant influence. Figure 10a shows the correlations of NC and LC at a W/B ratio of 0.41. The correlation coefficient (R^2) was found to be 0.94 for NC41 and 0.98 for LC41. When the ultrasonic pulse velocity was lower than 2.2 km/s, the graph of NC41 was approximately 5% higher, whereas above 2.2 km/s, the graph of LC41 became higher. The difference between NC41 and LC41 was approximately 7% in the 2.2–2.5 km/s ultrasonic pulse velocity range, 12% in the 2.5–3 km/s range, 15% in the 3–3.5 km/s range, 17% in the 3.5–4 km/s range, and 18% in the range above 4.5 km/s.

Figure 10b shows the correlations of NC and LC at a W/B ratio of 0.33. The correlation coefficient (R^2) was found to be 0.95 for NC33 and 0.98 for LC33. Below 2.5 km/s, the graph of NC33 was approximately 12% higher, whereas above 2.5 km/s, the graph of LC33 became higher. The difference between NC33 and LC33 was approximately 7% in the 2.5–3 km/s range, 12% in the 3.0–3.5 km/s range, 15% in the 3.5–4.0 km/s range, and 17% in the range above 4.5 km/s. Relatively smaller differences occurred at the W/B ratio of 0.33 compared to those at 0.41.
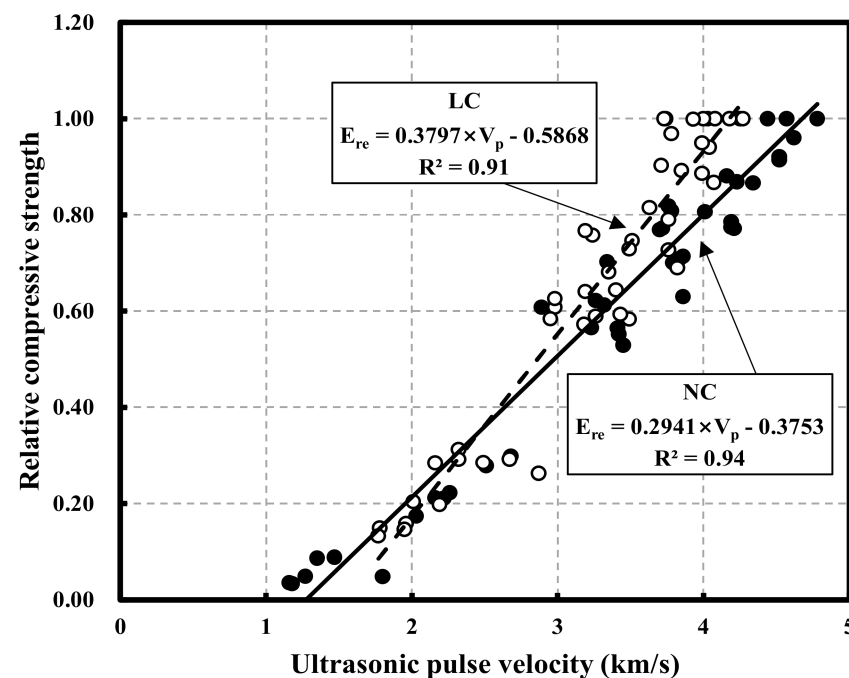
(a)

(b)

(c)

Figure 10. Correlation between ultrasonic pulse velocity and residual modulus of elasticity of normal concrete (NC) and lightweight concrete (LC) after high temperature exposure: (**a**) water-to-binder ratio (W/B) = 0.41; (**b**) W/B = 0.33; (**c**) W/B = 0.28.

Figure 10c shows the correlations of NC and LC at a W/B ratio of 0.28. The correlation coefficient (R^2) was 0.97 for NC28 and 0.94 for LC28. The graph of NC28 was approximately 30% higher in the 2.0–2.5 km/s range and 8% higher in the 2.5–3.0 km/s range than that of LC28. However, the graph of LC28 became higher in the higher range. The difference between NC28 and LC28 was approximately 4% in the 3.2–3.5 km/s range and 9% in the range above 3.5 km/s. In the very low ultrasonic pulse velocity range, the inside of the concrete may exhibit a similar state and stiffness because of the severe damage to the cement matrix. However, in the relatively higher range, it is deemed necessary to consider the aggregate type because it seems to be the dominant factor to influence the state of the paste–aggregate interface. Table 6 summarizes the correlation between the ultrasonic pulse velocity and residual modulus of elasticity.

Table 6. Correlation between ultrasonic pulse velocity and residual modulus of elasticity.

ID	Equation	Correlation Coefficient (R^2)
NC41	$E_{re} = 0.3174 \times V_p - 0.4014$	$R^2 = 0.94$
LC41	$E_{re} = 0.4158 \times V_p - 0.6108$	$R^2 = 0.98$
NC33	$E_{re} = 0.3144 \times V_p - 0.4471$	$R^2 = 0.95$
LC33	$E_{re} = 0.412 \times V_p - 0.6869$	$R^2 = 0.98$
NC28	$E_{re} = 0.2813 \times V_p - 0.3664$	$R^2 = 0.97$
LC28	$E_{re} = 0.3871 \times V_p - 0.6341$	$R^2 = 0.94$

Figure 11 shows the proposed prediction model of the residual modulus of elasticity vs. ultrasonic pulse velocity of the NC and LC after high temperature exposure (Table 7). In this study, equations for predicting the residual modulus of elasticity in the form of a linear function were proposed. A number of equations for the same have also been previously proposed [33–36]. NC exceeded LC by approximately 7% when the ultrasonic pulse velocity was lower than 2.5 km/s, but LC exceeded NC in the higher range. The difference between NC and LC was approximately 6% in the 2.5–3 km/s range, 11% in the 3–3.5 km/s range, 13% in the 3.5–4 km/s range, and 15% in the range above 4 km/s. This indicates that it is necessary to consider the aggregate type when predicting the residual modulus of elasticity of concrete through the analysis of the ultrasonic pulse velocity after high temperature exposure.

Figure 11. Proposed prediction model of residual modulus of elasticity vs. ultrasonic pulse velocity of normal concrete (NC) and lightweight concrete (LC) after high temperature exposure.

Table 7. Proposed equations using ultrasonic pulse velocities of normal concrete (NC) and lightweight concrete (LC) at elevated temperatures.

Derived Item	Concrete	Equation	Correlation Coefficient (R^2)
Residual modulus of elasticity	NC	$E_{re} = 0.2941 \times V_p - 0.3753$	$R^2 = 0.94$
	LC	$E_{re} = 0.3797 \times V_p - 0.5868$	$R^2 = 0.91$

4. Conclusions

In this study, the mechanical properties of NC and LC were analyzed at various W/B ratios after high temperature exposure. The experiment results are summarized as follows.

(1)   At all levels, the residual compressive strength was reduced to approximately 0.86–0.91, which then slightly recovered at 300 °C. However, it continuously decreased at higher temperatures. At 700 °C, the residual compressive strength of LC appears to have improved compared to that of NC because of the influence of the aggregate.

(2)   The ultrasonic pulse velocity and modulus of elasticity continued to decrease as the temperature increased, following a similar trend to that of the residual compressive strength. It is observed that the ultrasonic pulse velocity and modulus of elasticity improved for LC compared to NC, similar to compressive strength after high temperature exposure.

(3)   The slope of the stress–strain curve was similar to that of the curve before heating (20 °C) until 300 °C, but tended to decrease at temperatures higher than 300 °C. At high temperatures, LC showed a low peak strain at a relatively low stress compared to NC. This appears to be due to the relative low stiffness of the coarse aggregate in LC compared to that in NC.

(4)   Equations for predicting the residual modulus of elasticity through the analysis of the ultrasonic pulse velocity after high temperature exposure were proposed, with R^2 values of 0.94 and 0.941 for NC and LC, respectively.

In this study, contents on the prediction of strength through ultrasonic pulse velocity analysis after high temperature exposure in previous studies were examined. An attempt was made to propose a method for simultaneously predicting the strength and stiffness of concrete through a single ultrasonic pulse velocity measurement and analysis. As part of our future work, we intend to investigate material properties to produce various lightweight aggregates and acquire data on the mechanical properties of concrete at high temperatures.

Institutional Review Board Statement: Not applicable.

Informed Consent Statement: Not applicable.

Conflicts of Interest: The authors declare no conflict of interest. The funders had no role in the design of the study; in the collection, analyses, or interpretation of data; in the writing of the manuscript, or in the decision to publish the results.

References

1.   Kim, W.J.; Lee, H.S.K. Thermo-elastic analysis of reinforced concrete space frames by fiber model. *J. Korea Concr. Inst.* **2018**, *30*, 3–14. [CrossRef]
2.   Tae, S.H.; Lee, B.K. The effect of W/C ratio and chloride on compressive strength of concrete exposed to high-temperature. *J. Korean Soc. Saf.* **1998**, *14*, 124–128.
3.   Lee, J.W. Effect of elevated temperature on changes of color and residual compressive strength of concrete. *JAIK* **2011**, *27*, 35–42.
4.   Kim, Y.S.; Choi, H.G.; Ohmiya, Y.; Kim, G.Y. Effect of aggregate on mechanical properties of ultra-high strength concrete exposed to high temperature. *J. Korea Concr. Inst.* **2011**, *23*, 431–440. [CrossRef]
5.   Dolinar, D.; Trtnik, G.; Turk, G.; Hozjan, T. The feasibility of estimation of mechanical properties of limestone concrete after fire using nondestructive methods. *Constr. Build. Mater.* **2019**, *228*, 1167. [CrossRef]
6.   Arslan, M.H.; Erdogan, O.; Koken, A.; Erkan, I.H.; Dogan, G. Evaluation of fire performance of prefabricated concrete buildings in Turkey. *Mag. Concr. Res.* **2017**, *69*, 389–401. [CrossRef]

7. Chaix, J.F.; Garnier, V.; Corneloup, G. Concrete damage evolution analysis by backscattered ultrasonic waves. *NDT E Int.* **2003**, *36*, 461–469. [CrossRef]
8. Mohammadhosseini, H.; Alrshoudi, F.; Tahir, M.M.; Alyousef, R.; Alghamdi, H.; Alharbi, Y.R.; Alsaif, A. Performance evaluation of novel prepacked aggregate concrete reinforced with waste polypropylene fibers at elevated temperatures. *Constr. Build. Mater.* **2020**, *259*, 120418. [CrossRef]
9. Dias, A.R.O.; Amancio, F.A.; Rafael, M.F.C.; Cabral, A.E.B. Study of propagation of ultrasonic pulses in concrete exposed at high temperatures. *Procedia Struct. Integr.* **2018**, *11*, 84–90. [CrossRef]
10. Yang, H.; Lin, Y.; Hsiao, C.; Liu, J.Y. Evaluating residual compressive strength of concrete at elevated temperatures using ultrasonic pulse velocity. *Fire Saf. J.* **2009**, *44*, 121–130. [CrossRef]
11. Khan, E.U.; Khushnood, R.A.; Baloch, W.L. Spalling sensitivity and mechanical response of an ecofriendly sawdust high strength concrete at elevated temperatures. *Constr. Build. Mater.* **2020**, *258*, 119656. [CrossRef]
12. Comites Euro-International Du Beton. *Fire Design of Concrete Structures-In Accordance with CEB/FIP Model, Code 1991, 90*; Comites Euro-International Du Beton: Luxembourg, 1991.
13. Lee, K.S.; Candelaria, M.D.; Kee, S.H. Comparison of static and dynamic elastic moduli and compressive strength of concrete in two standard dry conditions: Oven dry and saturated-surface dry. *J. Korea Concr. Inst.* **2021**, *33*, 449–458. [CrossRef]
14. Hasan, M.; Saidi, T.; Afifuddin, M. Mechanical properties and absorption of lightweight concrete using lightweight aggregate from diatomaceous earth. *Constr. Build. Mater.* **2021**, *277*, 122324. [CrossRef]
15. Islam, M.M.U.; Li, J.; Wu, Y.; Roychand, R.; Saberian, M. Design and strength optimization method for the production of structural lightweight concrete: An experimental investigation for the complete replacement of conventional coarse aggregates by waste rubber particles. *Resour. Conserv. Recycl* **2022**, *184*, 106390. [CrossRef]
16. Kim, W.; Jeong, K.; Choi, H.; Lee, T. Correlation analysis of ultrasonic pulse velocity and mechanical properties of normal aggregate and lightweight aggregate concretes in 30–60 MPa range. *Materials* **2022**, *15*, 2952. [CrossRef] [PubMed]
17. *ASTM C1231/C1231-15*; Standard Practice for Use of Unbonded Caps in Determination of Compressive Strength of Hardened Cylindrical Concrete Specimens. American Society of Testing and Materials: West Conshohocken, PA, USA, 2016; pp. 1–5.
18. *ASTM C39/C39M*; Standard Test Method for Compressive Strength of Cylindrical Concrete Specimens. American Society of Testing and Materials: West Conshohocken, PA, USA, 2018; pp. 1–8.
19. *ASTM C469*; Standard Test Method for Static Modulus of Elasticity and Poisson's Ratio of Concrete in Compression. American Society of Testing and Materials: West Conshohocken, PA, USA, 2011; p. 469.
20. *ASTM C597-16*; Standard Test Method for Pulse Velocity Through Concrete. American Society of Testing and Materials: West Conshohocken, PA, USA, 2016; pp. 1–4.
21. Saridemir, M.; Celikten, S. Investigation of fire and chemical effects on the properties of alkali-activated lightweight concretes produced with basaltic pumice aggregate. *Constr. Build. Mater.* **2020**, *260*, 119969. [CrossRef]
22. *ASTM C642-13*; Standard Test Method for Density, Absorption, and Voids in Hardened Concrete. ASTM International: West Conshohocken, PA, USA, 2013.
23. Dinakar, P.; Babu, K.G.; Santhanam, M. Durability properties of high volume fly ash self-compacting concretes. *Cem. Concr. Compos.* **2008**, *30*, 880–886. [CrossRef]
24. Yoon, M.H.; Choe, G.C.; Lee, T.G.; Kim, G.Y. Evaluation on strain properties of 60 MPa class high strength concrete according to the coarse aggregate type and elevated temperature condition. *J. Korea Concr. Inst.* **2014**, *26*, 247–254. [CrossRef]
25. Andic-Cakir, O.; Hizal, S. Influence of elevated temperatures on the mechanical properties and microstructure of self-consolidating lightweight aggregate concrete. *Constr. Build. Mater.* **2012**, *34*, 575–583. [CrossRef]
26. Roufael, G.; Beaucour, A.-L.; Eslami, J.; Hoxha, D.; Noumowe, A. Influence of lightweight aggregates on the physical and mechanical residual properties of concrete subjected to high temperatures. *Constr. Build. Mater.* **2021**, *268*, 121221. [CrossRef]
27. Toric, N.; Boko, I.; Juradin, S.; Baloevic, G. Mechanical properties of lightweight concrete after fire exposure. *Struct. Concr.* **2016**, *17*, 1071–1081. [CrossRef]
28. Vieira, J.P.B.; Correja, J.R.; de Brito, J. Post-fire residual mechanical properties of concrete made with recycled concrete coarse aggregates. *Cem. Concr. Res.* **2011**, *41*, 533–541. [CrossRef]
29. Choe, C.C.; Kim, G.Y.; Kim, H.S.; Hwang, E.C.; Nam, J.S. Mechanical properties of amorphous steel fiber reinforced high strength concrete exposed to high temperature. *J. Korea Concr. Inst.* **2020**, *32*, 19–26. [CrossRef]
30. Choe, G.C.; Min, M.H.; Lee, T.G.; Lee, S.H.; Kim, G.Y. Evaluation of properties of 80, 130, 180 MPa high strength concrete at high temperature with heating and loading. *Constr. Build. Mater.* **2013**, *25*, 613–620.
31. Lee, T.; Jeong, K.; Choi, H. Effect of thermal properties of aggregates on the mechanical properties of high strength concrete under loading and high temperature conditions. *Materials* **2021**, *14*, 6093. [CrossRef] [PubMed]
32. Chang, Y.F.; Chen, Y.H.; Sheu, M.S.; Yao, G.C. Residual stress–strain relationship for concrete after exposure to high temperatures. *Cem. Concr. Res.* **2006**, *36*, 1999–2005. [CrossRef]

33. Verma, D.; Kainthola, A.; Singh, R.; Singh, T.N. Assessment of geo-mechanical properties of some Gondwana coal using P-Wave velocity. *Int. Res. J. Geol. Min.* **2012**, *2*, 261–274.

34. Khandelwal, M.; Singh, T.N. Correlating static properties of coal measures rocks with P-wave velocity. *Int. J. Coal Geol.* **2009**, *79*, 55–60. [CrossRef]

35. Chawre, B. Correlations between ultrasonic pulse wave velocities and rock properties of quartz-mica schist. *J. Rock Mech. Geotech. Eng.* **2018**, *10*, 594–602. [CrossRef]

36. Brotons, V.; Tomas, R.; Ivorra, S.; Grediaga, A.; Martinez-Martinez, J.; Benavente, D.; Gomez-Heras, M. Improved correlation between the static and dynamic elastic modulus of different types of rocks. *Mater. Struct.* **2016**, *49*, 3021–3037. [CrossRef]